Observations and the source investigations of boundary layer BrO in Ny-Ålesund Arctic

Yuhan Luo[1], Fuqi Si[1], Haijin Zhou[1], Ke Dou[1], Yi Liu[2] and Wenqing Liu[1]

[1]Anhui Institute of Optics and Fine Mechanics, Chinese Academy of Sciences, Hefei, 230031, China

5 [2]National Synchrotron Radiation Laboratory, University of Science and Technology of China, Hefei, 230027, China

Correspondence to: Yuhan Luo (yhluo@aiofm.ac.cn) and Fuqi Si (sifuqi@aiofm.ac.cn)

Abstract. During polar spring, the presents of reactive bromine in polar boundary layer are considered as the main cause of the ozone depletion and mercury deposition. But many uncertainties still remain in understanding the mechanisms of the chemical process and the source of bromine. As the Arctic sea ice has dramatically reduced recently, 10 it is critical to investigate the mechanism using more accurate measurements with higher temporal and spatial resolution. In this study, a typical process of enhanced bromine and depleted ozone in late April, 2015 in Ny-Ålesund boundary layer was observed applying ground-based Multi Axis-Differential Optical Absorption Spectroscopy (MAX-DOAS) technique. The results showed that there were as high as 5.6×10^{14} molecular cm^{-2} BrO slant columns above the Kings Bay area in 26 April. Meanwhile, the boundary layer ozone and gaseous elemental mercury (GEM) 15 was synchronously reduced by 85% and 90% respectively. Considering meteorology, sea ice distribution and air mass history, the sea ice in the Kings Bay area, emerged only for a very short period time when the enhance BrO was observed, was considered as the major source of this bromine enhancement event. The kinetic calculation showed that the ozone loss rate is 10.3 ppbv h^{-1}, which is extremely high compared to other area. The GEM loss rate is about 0.25 ng m^{-3} h^{-1}. The oxidized GEM may directly deposit to snow/ice and thereby influence the polar ecosystem.

20 **1 Introduction**

Bromine monoxide is one of the key reactive halogen species which have profound impacts on the atmosphere chemistry of the polar boundary layer (PBL), especially the oxidative capacity of the troposphere (Saiz-Lopez and von Glasow, 2012). The presence of reactive bromine (in some situations "bromine explosion") is considered as the main cause of the depletion of boundary layer ozone, called "ozone depletion events" (ODEs) (Platt and Hönninger, 2003). 25 Furthermore, halogens can efficiently oxidize gas-phase mercury, which can lead to a decrease of gaseous mercury, called "atmospheric mercury depletion events (AMDEs)" (Ariya et al., 2002;Ariya et al., 2004;Lindberg et al., 2002;Lu et al., 2001;Steffen et al., 2008). Enhanced BrO was firstly detected by Long Path Differential Optical Absorption Spectroscopy (LP-DOAS) observations (Platt, 1994). Satellite measurements confirmed that the phenomenon of bromine enhancement covers larger area of polar regions by deriving daily global BrO map (Richter et

al., 1998);(Platt and Wagner, 1998;Wagner et al., 2001;Sihler et al., 2013).The primary source of reactive bromine has been explained by a series of photochemical and heterogeneous reactions at the surface of frozen ocean during polar spring (Fan and Jacob, 1992). A typical heterogeneous reaction model between gaseous and condensed phases was shown in Fig.1. Bromine is released from salty ice surfaces to the atmosphere in an autocatalytic chemical mechanism that oxidizes bromide to reactive bromine. The reaction of HOBr in aerosol is proposed to be the pivot to explain the recycling reaction, which is an acid-catalyzed reaction (Simpson et al., 2007). Sea-ice (first year) surfaces, brine, and frost flowers have been considered as possible source of bromide aerosols (Kaleschke et al., 2004) (Lehrer et al., 2004).

However, the true circumstance is that the ODEs and BrO enhancement are not always in consistency. There are only few reports of Arctic ODEs that are assumed to have been observed primarily as a result of local-scale chemical mechanism (Bottenheim et al., 2009;Jacobi et al., 2006). As the photochemical reactions are quickly happened and the lifetime of the intermediate products, e.g. the reactive bromine radicals are quite short, more accurate data with higher temporal resolution are needed to analyzing chemical process in PBL and investigating source of bromine.

MAX-DOAS (Multi-AXis Differential Optical Absorption Spectrometer) technique has the advantage of being able to separate clearly the tropospheric and stratospheric portions of the atmospheric column, and even derive a crude vertical profile (Frieß et al., 2011). When pointing to a direction slightly above the horizon, high sensitivities for the trace gases close to the ground can be obtained due to the long light path through the trace gas layers. It is also an important calibration of satellite observations, which has lower spatial and temporal resolution compared with ground-based measurements. In the Arctic area, ground-based MAX-DOAS observations have been made at Barrow, Alaska (71 °N, 157 °W), Alert, northern Canada (82.5 °N, 62.3 °W) and Ny-Ålesund, Svalbard (78.9 °N, 11.8 °E) (Tab.1). Besides, air-borne (Neuman et al., 2010;Pöhler et al., 2013) and ship-borne measurements (Bottenheim et al., 2009;Jacobi et al., 2006;Leser et al., 2003;Wagner et al., 2007) are important supplements for the analysis and modelling of bromine chemistry.

However, recently the Arctic sea ice coverage has dramatically reduced, especially at East Greenland and North of Europe. Influenced by the North Atlantic Warm Current (NAWC), the near surface air temperature and sea surface temperature (SST) are getting higher at North Europe (Fig.2). In recent years, Kings Bay in Ny-Ålesund has ice-free open water all year round, which is a unique character comparing with other parts at the same latitude in Arctic. Therefore, it is critical to have a better understanding of the possible reactive bromine source and the impact of the halogen activation on PBL ozone depletion and mercury deposition under a rapidly change Arctic. In this study, we have caught a unique process of enhanced bromine and depleted ozone in Ny-Ålesund in late April. The key role of bromine was confirmed by ground-based MAX-DOAS measurements. This event provides a rare opportunity to investigate the source of bromine and process of ozone depletion at this area. Kinetic studies of ozone depletion and

gaseous mercury deposition are discussed afterwards.

2 Instruments and methods

2.1 Instrument setup

The MAX-DOAS measurement site is located at Yellow River Station (78°55′30"N, 11°55′20"E) at Ny-Ålesund, west coast of Spitsbergen. The observation position is shown in Fig. 3. To have a rough idea of the climate condition, monthly mean sea ice concentrations anomalies and air temperature anomalies in April 2015 are demonstrated in Fig. 2. The observations were carried out from 25 April to 15 May 2015. Due to the wavelength adjustment, no data is available during a short period from 28 to 29 April.

The MAX-DOAS instrument operated at Ny-Ålesund consists of indoor and outdoor parts. The telescope receiving scattered sunlight from multi angles is controlled by a stepper motor to adjust elevation angles from horizon (0°) to zenith (90°). The field of view of the telescope is about 1°. The scattered sun light is imported through the quartz fiber with numerical aperture of 0.22 into the indoor spectrograph (Ocean Optics MAYA pro) with a one dimensional CCD (ILX511 linear array CCD) containing 2068 pixels. The wavelength range of the spectrograph is from 290 nm to 420 nm, thus enabling the analysis of trace gases including O_3, NO_2, BrO, OClO, HCHO, and O_4. The spectral resolution is about 0.5nm (FWHM). The CCD detector is cooled at -30℃ while the whole spectrometer is thermally stabilized at +20℃ using a thermal controller. A computer sets the configuration of the system and controls the automatic measurements. The integration time (typically from 100 ms to 2000 ms multiple 100 scan times) of each measurement depends on the intensity of scattered light which can be influenced by cloud and visibility. The standard mercury lamp is used for spectra calibration. Calibration measurements of dark current and offset are performed after each measurement.

The telescope is pointed towards Northeast direction, which covers the Kings Bay area (Fig.3). Kings Bay is an inlet on the west coast of Spitsbergen, one part of the Svalbard archipelago in the Arctic Ocean. The inlet is 26 km long and 6 to 14 km wide. The range of MAX-DOAS measurement is about 10km radius area, which covers the central area of the fjord. The sequence of elevation angles is 2°, 3°, 4°, 5°, 6°, 8°, 10°, 15°, 30° and 90° above the horizon.

2.2 Data evaluation

The spectra measured with the above described setup are analyzed using the well-established DOAS retrieving method (Platt, 1994). The wavelength calibration was performed using the QDOAS software developed by the Belgian Institute for Space Aeronomy (BIRA) by fitting the reference spectrum to a high resolution Fraunhofer spectrum (Kurucz et al., 1988). The spectral analysis of BrO is performed at 340-359 nm, encompassing three BrO absorptions

bands, which improves the accuracy of the inversion. O_3 (223K, 243K) (Bogumil et al., 2003;Vandaele et al., 1998), NO_2 (298K, 220K) (Vandaele et al., 1998), O_4 (Hermans et al., 2003), BrO (228K) (Wilmouth et al., 1999), OClO (233K) (Kromminga et al., 2003), and Ring Structure (Chance and Spurr, 1997) are involved in the inversion algorithm. The O_4 retrieval is performed using the same set of cross sections as for BrO but in the wavelength interval at 340-370

5 nm. The high resolution cross sections were convoluted with the instrument slit function determined by measuring the emission line of a mercury lamp. A fifth order of polynomial was applied to eliminate the broad band structures in the spectra caused by Rayleigh and Mie scattering. Furthermore, a nonlinear intensity offset was included in the fit to account for possible instrumental stray light. A wavelength shift and stretch of the spectra was allowed in the fit in order to compensate for small changes in the spectral adjustment of the spectrograph.

10 The fit procedure yields differential slant column densities (dSCD) using noon time zenith sky measurements as Fraunhofer reference for the analysis. An example of the fit result of BrO and O_4 is shown in Fig.4. The spectrum was recorded on 26 April, 2015 19:59 UTC (SZA=86 °) at the elevation angle of 2 °. The BrO dSCD is 5.10×10^{14} molecular cm^{-2}. The residual root mean square is 4.59×10^{-4}, resulting in a statistical BrO dSCD error of 1.63×10^{13} molecular cm^{-2}. The DSCDs of BrO at elevation angle 2 ° were obtained by subtracting 90 °of each sequence, which eliminate the

15 influence of stratosphere BrO change.

Since DSCDs are dependent on the light path, wavelength and observation geometry, DSCDs are then converted to vertical column density (VCD) by dividing the differential air mass factor (DAMF), which is the averaged light path enhancement for solar light traveling through the atmosphere compared to a straight vertical path.

We perform the radiative transfer modeling (RTM) simulations using SCIATRAN (Rozanov et al., 2005) to get

20 modeled DAMF using five different assumed BrO profiles with evenly distributed air masses: a. 0-0.5 km; b. 0-1 km; c. 0-2 km; d. 0.5-1 km; e. 1-2 km (Fig.5a). The models are performed under clear sky condition with no aerosol input. Remarkable difference exists for different input profiles. For BrO layer 0-0.5km, 0-1 km and 0-2 km, DAMFs all increase with the decrease of elevation angles. While for BrO layer 0.5-1 km and 1-2 km, the dependence on the telescope elevation angle is weaker especially at small elevation angles.

25 The modeled BrO SCDs for different input BrO profiles are shown in Fig.5b. The input BrO VCD is 5×10^{13} molecules/cm^2. The measured BrO SCDs from 20:00 26/04 to 05:00 27/04 are also plotted. The blue dots indicate data points for the first 4 hours in 26/04, while red and orange dots indicate later 4 hours in the morning of 27/04. BrO layer between 0-1 km can be considered as the most possible distribution of BrO layer, which is compatible with the measurements. Thereby, BrO SCDs can be converted to volume mixing ratios (*VMR*) assuming a homogeneous BrO

30 layer of 1 km thickness at the surface.

2.3 Complementary data

Ny-Ålesund is a science community hosting over fifteen permanent research stations. Atmospheric measurements have been measured continuously at Zeppelin Station, Ny-Ålesund since 1990. Located on Zeppelin Mountain with altitude 474 meters a.s.l., it is a background atmosphere observatory operated by NPI (Norwegian Polar Institute) and NILU
5   (Norwegian Institute for Air Research) , which are part of the Global Atmosphere Watch (GAW) Framework.

Surface ozone was measured by UV photometry. Gaseous mercury in air was measured using Tekran mercury detector. Hourly Surface Ozone and gaseous mercury data are downloaded at EBAS database (Tørseth et al., 2012).

Meteorology data including temperature, air pressure, relative humidity, wind direction and velocity, and global radiation are recorded by AWIPEV Atmospheric Observatory in Ny-Ålesund. According to the sondes records of
10   temperature, humidity and wind speed from AWIPEV, the height of the troposphere is around 8000 meters and the height of boundary layer is around 1200 meters at Ny-Ålesund.

Webcam on the 474m Zeppelin Mountain records the sea ice change of Kings Bay and the cloud situation of Ny-Ålesund. (https://data.npolar.no/_file/zeppelin/camera/)

In order to get a rough idea of BrO distribution, BrO maps of northern hemisphere by GOME-2 product are
15   downloaded from http://www.iup.uni-bremen.de/doas/scia_data_browser.htm. Stations overpass BrO vertical column densities for MetOp-A (GOME-2A) and MetOp-B (GOME-2B) in Ny-Ålesund, Arctic are downloaded from https://avdc.gsfc.nasa.gov/index.php?site=580525926&id=97.

Using Hybrid Single-Particle Lagrangian Integrated Trajectory (HYSPLIT) model via the NASA ARL READY website (http://www.ready.noaa.gov/ready/open/hysplit4.html) (Draxler and Rolph, 2013;Stein et al., 2015), back
20   trajectory analyses were carried out to find the history of air masses. 72-hours ensemble back trajectories were driven by meteorological fields from the NCEP Global Data Assimilation System (GDAS) model output.

3 Results

Time series of BrO DSCDs at 2°, surface ozone concentrations, solar zenith angle (SZA), air pressure, air temperature, relative humidity, wind velocity and wind direction from 25 April to 15 May are presented in Fig.6. Starting from late
25   afternoon in 26 April, BrO DSCDs clearly exceeded the background levels and peaked at 5.6×10^{14} molecular cm^{-2}. At the same period, surface ozone sharply decreased to several ppb and not recovered to normal value until 29 April. During this period, the wind velocity is more than 5 m/s and decreases in 29 April. Over a period of one week, elevated BrO levels went back to the detection limit in 4 May under a stable boundary layer. During 4-5 May, partial ozone (not to near zero level) was depleted in the absence of BrO.
30   Time series of BrO dSCDs from 26 April to 28 April in every elevation angle (2°, 3°, 4°, 6°, 8°, 10°, 15°, 30°) are

plotted in Fig. 7. Results of different elevation angles distinguished obviously during the BrO enhancement period. But the differences of the BrO dSCDs ≤4 ° are very small, indicating that the highest value of BrO is probably not above the surface. In order to have a better understanding of the vertical distribution of reactive bromine at Arctic boundary layer, comparison between the measured BrO SCDs from MAX-DOAS measurements with the modeled ones from SCIATRAN model are performed (Fig.5). BrO layer height between 0-1 km is considered as the most possible distribution of BrO layer, which is compatible with the measurements. BrO dSCDs distributed from 0-1 km to more likely at 0.5-1 km along with time. This could be explained by that Br/BrO photochemistry reactions are taking place from the boundary layer to the free troposphere where there is enough ozone to react.

Sunshine duration, global radiation, SZA, BrO DSCDs from MAX-DOAS at 2 ° elevation angle, BrO volume mixing ratio, surface ozone and gaseous mercury from 26-28 April are plotted in Fig. 8. The BrO VMRs were calculated assuming a 0-1 km layer of BrO profile. The highest BrO VMR is about 15 pptv during the ODE. Ozone as well as gaseous mercury dropped extremely fast right after the enhancement of BrO. But there seems not sufficient reactive bromine presented locally in the boundary layer since the ozone turned to slowly increase just four hours later (at 23:00 26 April). Afterwards, both ozone and mercury has a slowly recovery with a fluctuation in the 27 afternoon.

4 Discussions

In this research, high concentration of troposphere BrO has been detected using the ground-based MAX-DOAS technique. As high as 5.6×10^{14} molecular cm^{-2} BrO column has been detected above Kings Bay, Ny-Ålesund. The retrieval shows that the enhancement occurred accompanied with severe ozone depletion and mercury deposition. This enhancement event is a good opportunity to investigate the source of BrO and the impact on the environment of Arctic boundary layer. The following parts are discussed in detail from air mass history, sea ice distribution, and ozone loss and mercury deposition.

4.1 History of air masses

Possible sources of reactive bromine are newly formed sea ice and frost flowers which can provide highly concentrated saline surfaces, thereby adequate sea salt aerosols. Another important source is the transport of the air masses which already contain elevated BrO and depleted ozone. Therefore, we investigate the history of the air masses arriving at measurement site using backward trajectories. Furthermore, the sea ice distribution (Fig.2) and the satellite BrO maps (Fig.10) are important instructions as well.

72-hour backward trajectories at Ny-Ålesund (10, 500, 1000 meters a.s.l.) from 26 April (0600 UTC) to 27 April (1800 UTC) were calculated every 6 hours (Fig.9). From the map of three altitudes, air masses turned from northwest

direction, which is origin from North America to the middle of Arctic Sea. From the vertical distribution of air masses, before noon of 26 April, the air masses came from low boundary layer, while after 18:00 26 April, from the upper troposphere.

BrO VCD map from GOME-2 measurements from 20 April to 13 May 2015 are shown in Fig. 10. BrO clouds existed at two main periods: coastal North America and Chukchi Sea during 22-23 April and North of Siberia during 08-11 May 2015. Both of the BrO clouds lasted about three to four days, the first of which was occasionally at the same period with the Ny-Ålesund BrO enhancement event. However, what we found by ground-based MAX-DOAS just lasted for several hours, which is at different time scale. Thereby, air masses transported from high latitude of Arctic from 22 April might have an impact on BrO enhancement in Ny-Ålesund, but not the most critical reason. Additionally, the transport air masses might be the reason of the slowly back BrO concentrations to normal values until 3 May.

4.2 Sea ice distribution

According to the observation of sea ice concentration from AMSR-E and Zeppelin webcam, Kings Bay is ice-free water area during the measurement period. However, large amount of sea ice appeared at Kings Bay on 26 April (Fig.11), floating from the bay entrance by both wind and tidal and lasted for few hours. The shape of sea ice was broken ice pieces with irregular border. The ice–sea water mixture was filled in the gaps, which was salty-enriched.

The efficient ozone loss is consistent with the temperature decline (Fig.12). The meteorology data shows that on 26 April air temperature continually goes down and reaches bottom of -11.4^{o}C at 22:00. According to the precipitation curve of calcium carbonate, more than 80% of carbonate precipitates below 265K. This process will provide acid aerosol from alkaline sea water, which triggers the transformation of inert sea-salt bromide to reactive bromine (Sander et al., 2006). Although the sun radiation intensity is not strong at that time, the heterogeneous reactions can still happen under the twilight.

Thereby, this BrO enhancement event is more likely a local process, mainly influenced by underlying surface change and local environment. The surface ozone concentrations increased along with the melting of sea ice, which indicated that the life span of BrO radicals are very short. When sea ice disappeared, the reaction immediately ended and reactive bromine radicals gradually transformed to soluble bromide (e.g. HOBr), which explained the sink of it (Fan and Jacob, 1992).

4.3 Kinetic analysis

What makes this case very special is that the increasing rate of BrO and the depletion rate of boundary layer ozone are

really fast. The surface ozone reduced by 85% within 4 hours. The ozone loss rate is as high as 10.3 ppbv h[-1] or 248 ppbv d[-1], which is extremely high compared with previous studies in Polar Regions (Tab. 2). The deposition of gaseous mercury occurred concurrently with tropospheric ozone depletion, as well as the enhancement of BrO (Fig. 14), which indicated that the oxidation of GEM by reactive halogen species (Br atoms and BrO radicals) is considered to be the key process of mercury depletion. The GEM decreases from ~2 ng m^{-3} to lower than 0.3 ng m^{-3} during the BrO enhancement event. The mercury loss rate is about ~0.25 ng m^{-3} h^{-1} or 6 ng m^{-3} d^{-1}. The oxidized GEM may directly deposit to snow/ice or associate with particles in the air that can subsequently deposit onto the snow and ice surfaces, and thereby threaten polar ecosystems and human health.

The chemical kinetics of bromine enhancement and ozone decay are analyzed assuming that the catalytic reactions are dominated by reactions showed in Fig.1. A first-order loss of ozone is due to reaction $Br+O_3 \rightarrow BrO+O_2$ resulting in the rate law:

$$r = -\frac{d[O_3]}{dt} = k_1 \cdot [O_3] \qquad \text{(Eq. 1)}$$

$$[O_3] = [O_3]_0 \cdot \exp(-k_1 \cdot t) \qquad \text{(Eq. 2)}$$

$$\ln\frac{[O_3]}{[O_3]_0} = -k_1 \cdot t \qquad \text{(Eq. 3)}$$

$[O_3]_0$ is the ozone concentration at the beginning of decay determined from the measured mixing ratio of 74.72 ppbv. $\ln\frac{[O_3]}{[O_3]_0}$ versus time are showed as hollow square in Fig. 13a.

According to the method by Jacobi et al. (Jacobi et al., 2006), the first order rate constant k_1 can be determined as follows:

$$\frac{d(\ln\frac{[O_3]}{[O_3]_0})}{dt} = -k_1 \qquad \text{(Eq. 4)}$$

The measured decrease of $\ln\frac{[O_3]}{[O_3]_0}$ versus time was fitted by:

$$\ln\frac{[O_3]}{[O_3]_0} = -\exp(b \cdot t + a) \qquad \text{(Eq. 5)}$$

$$\frac{d(\ln\frac{[O_3]}{[O_3]_0})}{dt} = -b \cdot \exp(b \cdot t + a) \qquad \text{(Eq. 6)}$$

$$\ln(-\ln\frac{[O_3]}{[O_3]_0}) = b \cdot t + a \qquad \text{(Eq. 7)}$$

$$k_1 = b \cdot \exp(b \cdot t + a) \qquad \text{(Eq. 8)}$$

$\ln(-\ln\frac{[O_3]}{[O_3]_0})$ versus time are plotted as black dots in Fig. 13a. The coefficients a and b are obtained from the linear fit in plot.

The ozone loss begins relatively slow and accelerates with time, which is consistent with the process of bromine explosion.

Assuming that the first order decay is dominated by the reaction $Br+O_3 \rightarrow BrO+O_2$, we are able to calculate the Br

concentrations as follows:

$$k_1 = k_{Br} \cdot [Br] \tag{Eq. 9}$$

$$k_{Br} = 1.7 \cdot 10^{-11} \cdot \exp(-\frac{800}{T}) \tag{Eq. 10}$$

k_{Br} is a constant depending on temperature (Fig. 13b). Thereby, the calculated Br concentration increases from 1.1×10^7 to about 1.2×10^9 atoms cm^{-3} (corresponding to 44.8 pptv) (Fig. 13c). Considering the assumption that the halogens are homogenously distributed in the PBL, the concentrations of Br at sea surface layer in the bromine explosion could be even higher.

5 Conclusions

Typical process of enhanced bromine and depleted ozone in Ny-Ålesund boundary layer was observed using ground based MAX-DOAS techniques in late April, 2015. As high as 5.6×10^{14} molecular cm^{-2} BrO DSCDs were detected on 26-27 April. Meanwhile, severe ozone depletion and mercury deposition occurred under BrO VMR of 15 pptv. The model showed enhanced BrO distributed at 0-1 km above the sea surface. By analyzing the air mass history and sea ice conditions, this BrO enhancement event is more likely a local process. The underlying sea ice and low temperature provide acid aerosols, which are prerequisites for the formation of BrO radicals. The kinetic analysis shows that the ozone loss begins relatively slow and accelerates with time, which is consistent with the process of bromine explosion. The ozone loss rate is as high as 10.3 ppbv h^{-1}, which is much higher than previous studies in Polar Regions. GEM loss rate is about ~0.25 ng m^{-3} h^{-1}. This study is a pivotal complement for BrO research in Arctic BL. Further observations and analysis are required to identify the chemical mechanisms.

Acknowledgements.

This research was financially supported by the National Natural Science Foundation of China Project No. 41676184, 41306199 and U1407135. We gratefully thank the Chinese Antarctic and Arctic Administration and the teammates of 2015 Chinese Arctic Expedition. We are also grateful to Dr. Ping Wang from KNMI and Dr. Yang Wang from MPIC for providing the advice on BrO VMR calculation. We kindly acknowledge the AWIPEV Atmospheric Observatory in Ny-Ålesund, the Norwegian Polar Institute and Norwegian Institute for Air Research (NILU) for the complementary data. Caroline Fayt, Thomas Danckaert and Michel van Roozendael from BIRA are gratefully acknowledged for providing the QDOAS analysis software. Meteorological data, surface ozone, and gaseous mercury were provided by EBAS database. Back trajectories were calculated using the HYSPLIT model from NOAA together with the GDAS data set from NCEP.

References

Ariya, P. A., Alexei Khalizov, A., and Gidas, A.: Reactions of gaseous mercury with atomic and molecular halogens: Kinetics,

product studies, and atmospheric implications, Journal of Physical Chemistry A, 106, 7310-7320, 2002.

Ariya, P. A., Dastoor, A. P., Marc, A., Schroeder, W. H., Leonard, B., Kurt, A., Farhad, R., Andrew, R., Didier, D., and Janick, L.: The arctic: A sink for mercury, Tellus, 56, 397-403, 2004.

Bogumil, K., Orphal, J., Homann, T., Voigt, S., Spietz, P., Fleischmann, O. C., Vogel, A., Hartmann, M., Kromminga, H., and Bovensmann, H.: Measurements of molecular absorption spectra with the sciamachy pre-flight model: Instrument characterization and reference data for atmospheric remote-sensing in the 230–2380 nm region, Journal of Photochemistry & Photobiology A Chemistry, 157, 167-184, 2003.

Bottenheim, J. W., Netcheva, S., Morin, S., and Nghiem, S. V.: Ozone in the boundary layer air over the arctic ocean: Measurements during the tara transpolar drift 2006-2008, Atmospheric Chemistry & Physics, 9, 4545-4557, 2009.

Chance, K. V., and Spurr, R. J. D.: Ring effect studies: Rayleigh scattering, including molecular parameters for rotational raman scattering, and the fraunhofer spectrum, Applied Optics, 36, 5224-5230, 1997.

Hysplit (hybrid single-particle lagrangian integrated trajectory) model access via noaa arl ready, 2013.

Fan, S. M., and Jacob, D. J.: Surface ozone depletion in arctic spring sustained by bromine reactions on aerosols, Nature, 359, 522-524, 1992.

Frieß, U., Hollwedel, J., König-Langlo, G., Wagner, T., and Platt, U.: Dynamics and chemistry of tropospheric bromine explosion events in the antarctic coastal region, Comptes Rendus Des Séances De La Société De Biologie Et De Ses Filiales, 109, 1454-1456, 2004.

Frieß, U., Sihler, H., Sander, R., Pöhler, D., Yilmaz, S., and Platt, U.: The vertical distribution of bro and aerosols in the arctic: Measurements by active and passive differential optical absorption spectroscopy, Journal of Geophysical Research Atmospheres, 116, 597-616, 2011.

Hönninger, G., and Platt, U.: Observations of bro and its vertical distribution during surface ozone depletion at alert, Atmospheric Environment, 36, 2481-2489, 2002.

Hebestreit, K., Stutz, J., Rosen, D., Matveiv, V. V., Peleg, M., Luria, M., and Platt, U.: Doas measurements of tropospheric bromine oxide in mid-latitudes, Science, 283, 55-57, 1999.

Hermans, C., Vandaele, A. C., Fally, S., Carleer, M., Colin, R., Coquart, B., Jenouvrier, A., and Merienne, M. F.: Absorption cross-section of the collision-induced bands of oxygen from the uv to the nir, Springer Netherlands, 193-202 pp., 2003.

Jacobi, H., Kaleschke, L., Richter, A., Rozanov, A., and Burrows, J. P.: Observation of a fast ozone loss in the marginal ice zone of the Arctic Ocean, Journal of Geophysical Research Atmospheres, 111, 3363-3375, 2006.

Kaleschke, L., Richter, A., Burrows, J., Afe, O., Heygster, G., Notholt, J., Rankin, A. M., Roscoe, H. K., Hollwedel, J., and Wagner, T.: Frost flowers on sea ice as a source of sea salt and their influence on tropospheric halogen chemistry, Geophysical Research Letters, 31, 371-375, 2004.

Kromminga, H., Orphal, J., Spietz, P., Voigt, S., and Burrows, J. P.: New measurements of oclo absorption cross-sections in

the 325-435 nm region and their temperature dependence between 213 and 293 k, Journal of Photochemistry & Photobiology A Chemistry, 157, 149-160, 2003.

Kurucz, R. L., Furenlid, I., Brault, J., and Testerman, L.: Solar flux atlas from 296 to 1300 nm, National Solar Observatory Atlas, Sunspot, New Mexico: National Solar Observatory, 1988.

5   Lehrer, E., Hönninger, G., and Platt, U.: A one dimensional model study of the mechanism of halogen liberation and vertical transport in the polar troposphere, Atmospheric Chemistry & Physics, 4, 2427-2440, 10.5194/acp-4-2427-2004, 2004.

Leser, H., Hönninger, G., and Platt, U.: MaxDOAS measurements of BrO and NO2 in the marine boundary layer, Geophysical Research Letters, 30, 149-164, 2003.

Lindberg, S. E., Brooks, S., Lin, C. J., Scott, K. J., Landis, M. S., Stevens, R. K., Goodsite, M., and Richter, A.: Dynamic

10   oxidation of gaseous mercury in the arctic troposphere at polar sunrise, Environmental Science & Technology, 36, 1245-1256, 10.1021/es0111941, 2002.

Lu, J. Y., Schroeder, W. H., Barrie, L. A., Steffen, A., Welch, H. E., Martin, K., Lockhart, L., Hunt, R. V., Boila, G., and Richter, A.: Magnification of atmospheric mercury deposition to polar regions in springtime: The link to tropospheric ozone depletion chemistry, Geophysical Research Letters, 28, 3219-3222, 2001.

15   Mcconnell, J. C., Henderson, G. S., Barrie, L., Bottenheim, J., Niki, H., Langford, C. H., and Templeton, E. M. J.: Photochemical bromine production implicated in arctic boundary-layer ozone depletion, Nature, 355, 150-152, 1992.

Neuman, J. A., Nowak, J. B., Huey, L. G., Burkholder, J. B., Dibb, J. E., Holloway, J. S., Liao, J., Peischl, J., Roberts, J. M., and Ryerson, T. B.: Bromine measurements in ozone depleted air over the arctic ocean, Atmospheric Chemistry & Physics, 10, 6503-6514, 2010.

20   Pöhler, D., Stephan, G., Zielcke, J., Shepson, P. B., Sihler, H., Stirm, B. H., Frieß, U., Pratt, K. A., Walsh, S., and Simpson, W. R.: Horizontal and vertical distribution of bromine monoxide in northern alaska during bromex derived from airborne imaging-doas measurements, EGU General Assembly Conference, 2013.

Platt, U.: Differential optical absorption spectroscopy (DOAS), in: Air monitoring by spectroscopic techniques, m.W. Sigrist, ed, Chem.anal.ser, 32, 327-333, 1994.

25   Platt, U., and Wagner, T.: Satellite mapping of enhanced bro concentrations in the troposphere, Nature, 395, 486-490, 1998.

Platt, U., and Hönninger, G.: The role of halogen species in the troposphere, Chemosphere, 52, 325, 2003.

Richter, A., Wittrock, F., Eisinger, M., and Burrows, J. P.: Gome observations of tropospheric bro in northern hemispheric spring and summer 1997, Geophysical Research Letters, 25, 2683-2686, 1998.

Rozanov, A., Rozanov, V., Buchwitz, M., Kokhanovsky, A., and Burrows, J. P.: Sciatran 2.0 - A new radiative transfer model

30   for geophysical applications in the 175-2400nm spectral region, Advances in Space Research, 36, 1015-1019, 2005.

Saiz-Lopez, A., Mahajan, A. S., Salmon, R. A., Bauguitte, S. J., Jones, A. E., Roscoe, H. K., and Plane, J. M.: Boundary layer halogens in coastal antarctica, Science, 317, 348-351, 2007.

Saiz-Lopez, A., and von Glasow, R.: Reactive halogen chemistry in the troposphere, Chemical Society Reviews, 41, 6448-6472, 10.1039/c2cs35208g, 2012.

Sander, R., Burrows, J., and Kaleschke, L.: Carbonate precipitation in brine – a potential trigger for tropospheric ozone depletion events, Atmospheric Chemistry & Physics, 6, 4653-4658, 2006.

Schroeder, W. H., Anlauf, K. G., Barrie, L. A., Lu, J. Y., Steffen, A., Schneeberger, Amp, D. R., and Berg, T.: Arctic springtime depletion of mercury, Nature, 394, 331-332, 1998.

Sihler, H., Platt, U., Frieß, U., Doerner, S., and Wagner, T.: Satellite observation of the seasonal distribution of tropospheric bromine monoxide in the arctic and its relation to sea-ice, temperature, and meteorology, EGU General Assembly 2013.

Simpson, W. R., Carlson, D., Nninger, G. H., Douglas, T. A., Sturm, M., Perovich, D., and Platt, U.: First-year sea-ice contact predicts bromine monoxide (BrO) levels at barrow, Alaska better than potential frost flower contact, Atmospheric Chemistry & Physics, 6, 11051-11066, 2007a.

Simpson, W. R., Glasow, R. V., Riedel, K., Anderson, P., Ariya, P., Bottenheim, J., Burrows, J., Carpenter, L. J., Frieß, U., and Goodsite, M. E.: Halogens and their role in polar boundary-layer ozone depletion, Atmospheric Chemistry & Physics, 7, 4375-4418, 2007b.

Sinreich, R., Merten, A., Molina, L., and Volkamer, R.: Parameterizing radiative transfer to convert max-doas dscds into near-surface box averaged mixing ratios and vertical profiles, Atmospheric Measurement Techniques, 5, 7641-7673, 2013.

Steffen, A., Douglas, T., Amyot, M., Ariya, P., Aspmo, K., Berg, T., Bottenheim, J., Brooks, S., Cobbett, F., and Dastoor, A.: A synthesis of atmospheric mercury depletion event chemistry in the atmosphere and snow, Atmospheric Chemistry & Physics, 8, 1445-1482, 2008.

Stein, A. F., Draxler, R. R., Rolph, G. D., Stunder, B. J. B., Cohen, M. D., and Ngan, F.: Noaa's hysplit atmospheric transport and dispersion modeling system, Bulletin of the American Meteorological Society, 96, 150504130527006, 2015.

Stutz, J., Thomas, J. L., Hurlock, S. C., Schneider, M., Glasow, R. V., Piot, M., Gorham, K., Burkhart, J. F., Ziemba, L., and Dibb, J. E.: Longpath doas observations of surface bro at summit, greenland, Atmospheric Chemistry & Physics, 11, 9899-9910, 2011.

Tørseth, K., Aas, W., Breivik, K., Fjæraa, A. M., Fiebig, M., Hjellbrekke, A. G., Lund Myhre, C., Solberg, S., and Yttri, K. E.: Introduction to the european monitoring and evaluation programme (emep) and observed atmospheric composition change during 1972–2009, Atmos. Chem. Phys., 12, 5447-5481, 10.5194/acp-12-5447-2012, 2012.

Tuckermann, M., Ackermann, R., Gölz, C., Lorenzen-Schmidt, H., Senne, T., Stutz, J., Trost, B., Unold, W., and Platt, U.: Doas observation of halogen radical atalysed arctic boundary layer ozone destruction during the arctoc ampaigns 1995 and 1996 in ny- lesund, spitsbergen, Tellus Series B-chemical & Physical Meteorology, 49, 533-555, 1997.

Vandaele, A. C., Hermans, C., Simon, P. C., Carleer, M., Colins, R., Fally, S., Merienne, M. F., Jenouvrier, A., and Coquart, B.: Measurements of the no2 absorption cross section from 42000cm-1 to 10000cm-1 (238-1000nm) at 220k and 294k,

J.quant.spectrosc.radiat.transfer, 59, 171-184, 1998.

Wagner, T., Leue, C., Wenig, M., Pfeilsticker, K., and Platt, U.: Spatial and temporal distribution of enhanced boundary layer bro concentrations measured by the gome instrument aboard ers-2, Journal of Geophysical Research Atmospheres, 106235, 225-224, 2001.

Wagner, T., Ibrahim, O., Sinreich, R., Frie, U., Glasow, R. V., and Platt, U.: Enhanced tropospheric bro over antarctic sea ice in mid-winter observed by max-doas on board the research vessel polarstern, Atmospheric Chemistry & Physics, 7, 3129-3142, 2007.

Wilmouth, D. M., Hanisco, T. F., And, N. M. D., and Anderson, J. G.: Fourier transform ultraviolet spectroscopy of the a 2e aF., And, N. M. D., and AndersonJ.phys.chem.a, 103, 8935-8945, 1999.

Table 1. Comparisons of BrO mixing ratio at four main Arctic observation sites

Sites	Observation periods	BrO mixing ratio	Methods	References
Greenland ice sheet **(72N, 38W, 3200ma.s.l.)**	14 May-15 June 2007, 9 June-8 July 2008	3-5ppt	LP-DOAS	(Stutz et al., 2011)
Barrow, Alaska **(71°19'N, 156°40'W)**	26 February-16 April 2009	~30ppt	MAX-DOAS LP-DOAS	(Frieß et al., 2011)
Alert, Nunavut **(82°32'N, 62°43'W)**	20 April- 9 May 2000	~30ppt	MAX-DOAS	(Hönninger and Platt, 2002)
Ny-Ålesund, Svalbard **(78.9N, 11.8E)**	20 April-27 April 1996	~30ppt	LP-DOAS	(Tuckermann et al., 1997)

Table 2. Comparisons of BrO mixing ratio and ozone loss rate

Method	BrO mixing ratio	Typ. Rate of O3 destruction	References
Observation at PBL	up to 30 pptv	1-2 ppbv h-1	(Tuckermann et al., 1997;Hönninger and Platt, 2002)
Observation at MIZ	~63 pptv	6.7 ppbv h-1 or 160 ppbv d-1	(Jacobi et al., 2006)
Observation at salt lakes	up to 176 pptv	10-20 ppbv h-1	(Hebestreit et al., 1999;Stutz et al., 2011)
Observation at Marine BL	~2 pptv	~0.05 ppbv h-1	(Leser et al., 2003)
Model	30-40 pptv	7.6 ppbv d-1	(Lehrer et al., 2004)
Model	100 pptv	40ppbv d-1	(Fan and Jacob, 1992)
Observation at Ny-Ålesund BL	~15 pptv	10.3 ppbv h^{-1} or 248 ppbv d^{-1}	**this study**
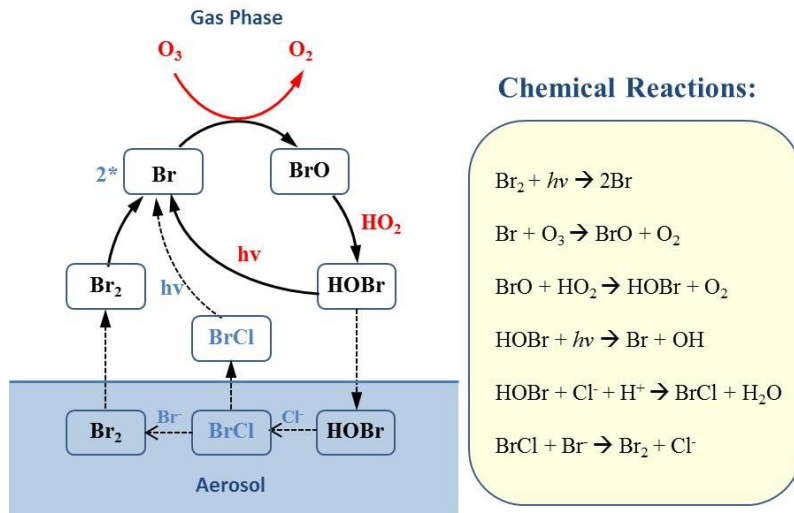
Fig. 1 Chemical reactions of BrO-Ozone cycle
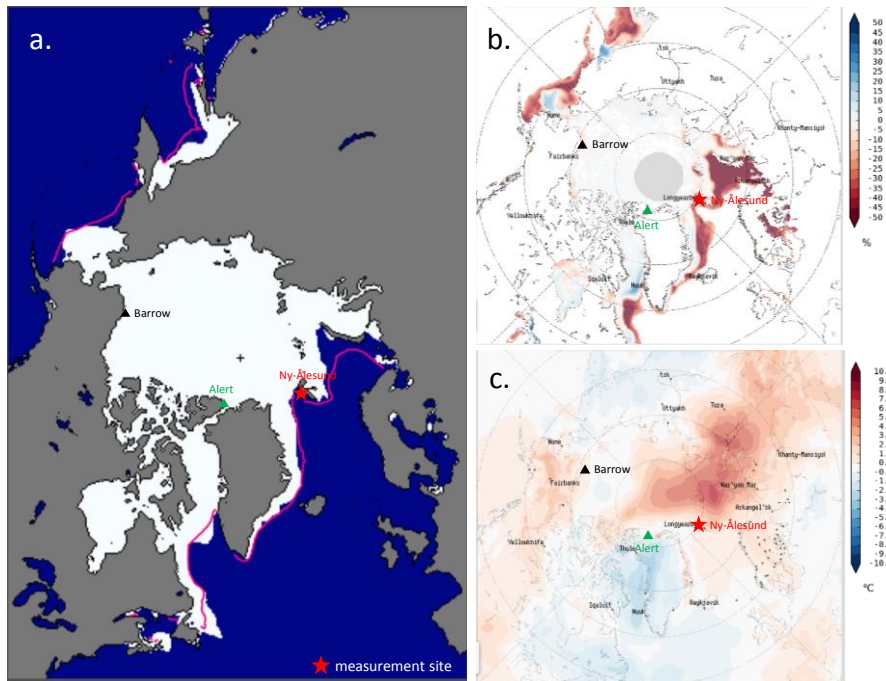
5   **Fig 2. a. Sea ice extent of Apr 2015 in Arctic area (data from http://nsidc.org/data/seaice_index/); b. Monthly mean sea ice concentrations anomalies of April 2015 compare to averages from 1979 to 2015 ; c. Two meters air temperature anomalies of April 2015 compare to averages from 1979 to 2015 (b and c data are from http://nsidc.org/soac)**
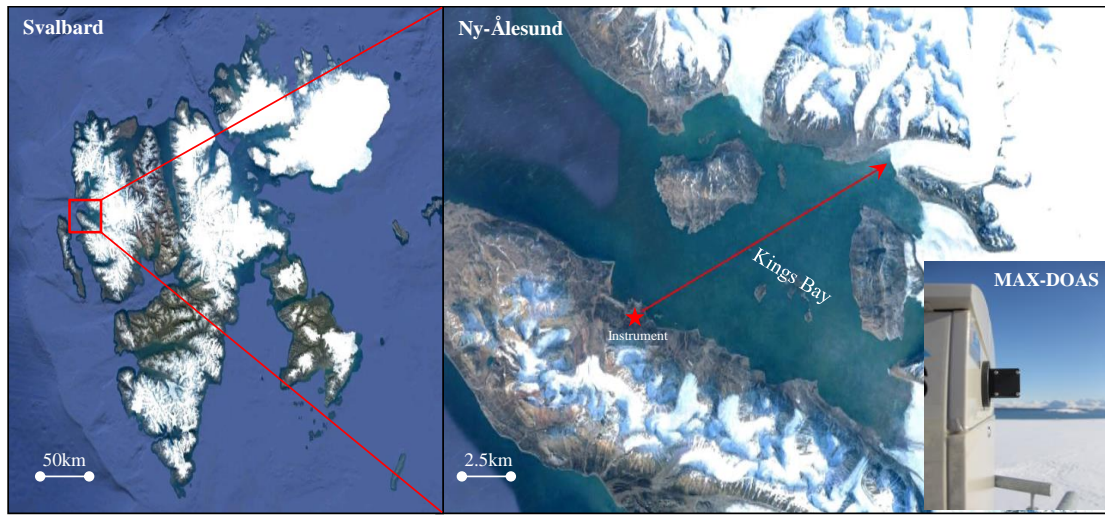
Fig.3 MAX-DOAS field observation in Ny-Ålesund, Arctic
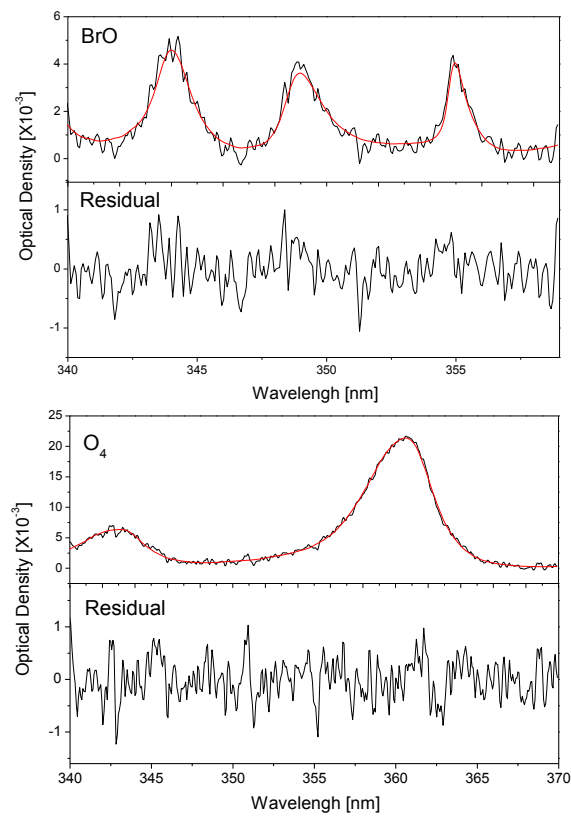
5   **Fig.4 Examples for spectral retrieval of BrO and O4. The spectrum was recorded under clear sky conditions at 2 ° elevation on 26 April 2015, 19:59 UTC, SZA = 86 °. (Black lines: Retrieved spectral signatures fitted result for absorber; red lines: fitted cross sections)**
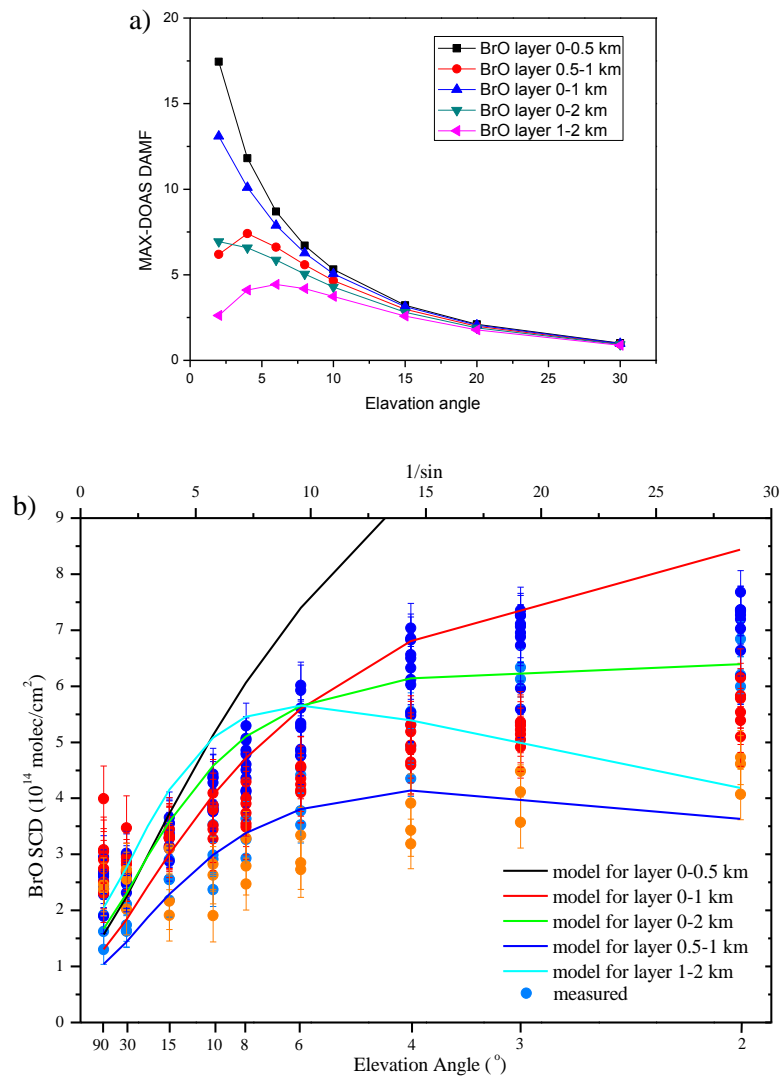
Fig. 5 The modeled DAMF (a) and BrO slant columns (b) using radiative transfer modeling simulation.
DAMF are the differences of AMF for low elevation angles and zenith direction. The models are performed assuming a clear sky
condition with no aerosol. In part b, the tropospheric BrO VCD is 5×10^{13} molecules/cm^2. The measured BrO SCDs during the
event are also shown (solid dots). The blue dots indicated data points from 20:00 to 24:00 in the evening of 26/04. The red and
orange dots indicated data points from 00:00-4:00 in the morning of 27/04.
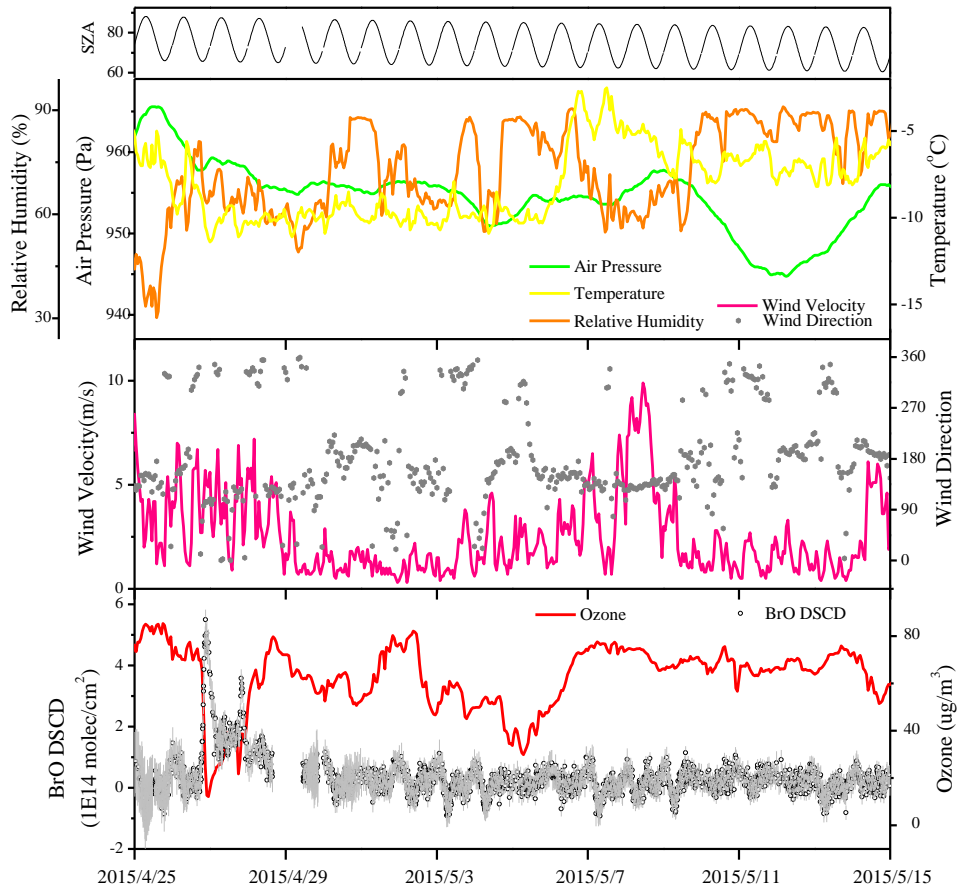
Fig.6 Time series of BrO dSCDs at 2 °, surface ozone, SZA and meteorology data during the measurement.
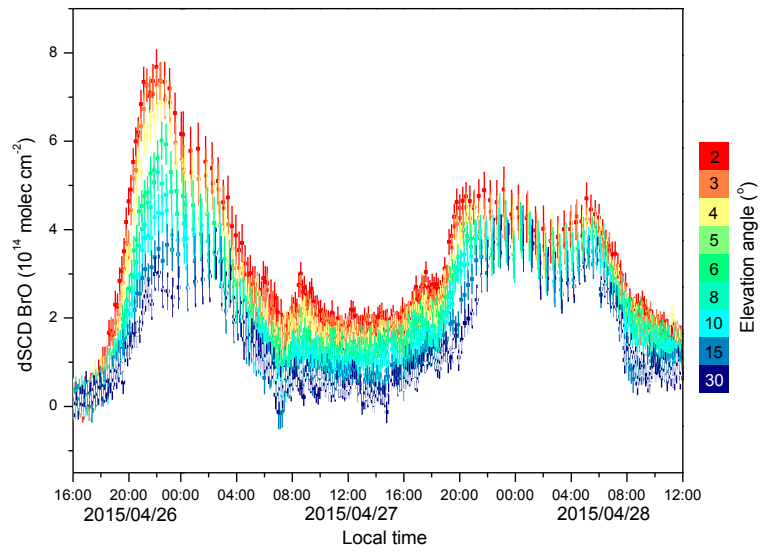
5 **Fig.7 BrO dSCDs of different elevation angles during the enhancement period**
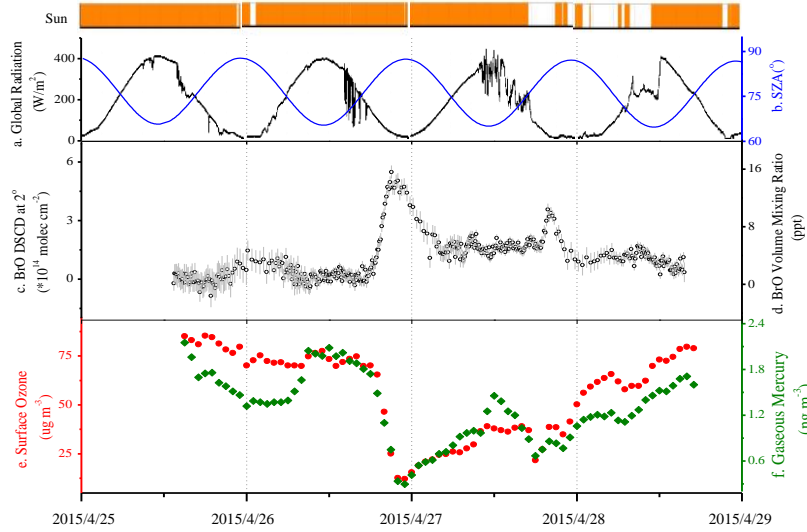
Fig.8 a. Global radiation (W/m^2) (Cited from AWIPEV database); b. SZA; c. BrO DSCDs from MAX-DOAS at elevation angle 2 $^\circ$; d. BrO VMR (ppt); e. surface ozone (ug/m^3); and f. gaseous mercury (ng/m^3) from 25/04 noon to 28/04 2015. BrO mixing ratios are calculated assuming a homogeneous BrO layer of 0-1 km.
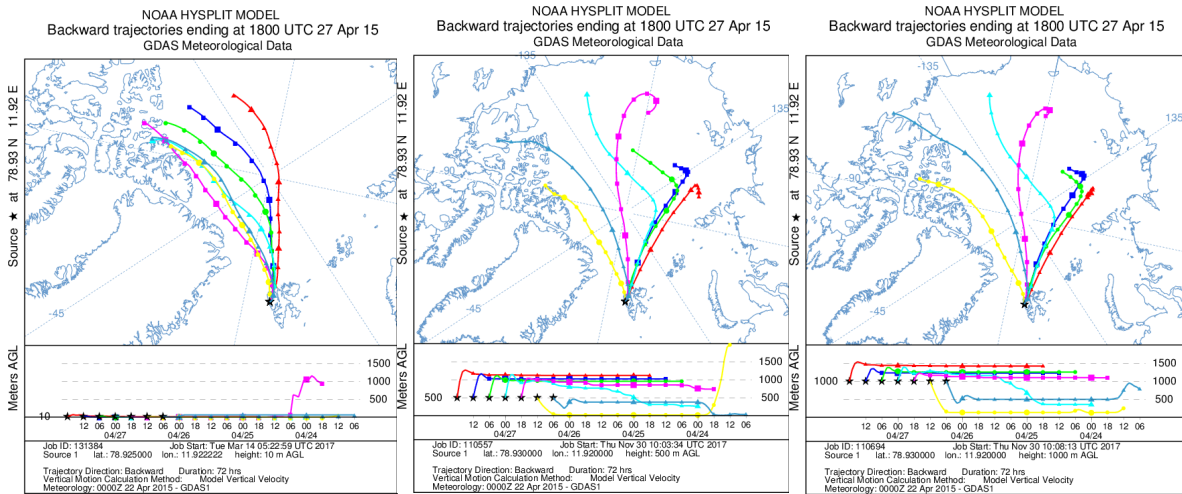
Fig. 9 Back trajectory model of air masses arriving at Ny-Ålesund from 26 April (0600 UTC) to 27 April (1800 UTC) at 10, 500, 1000 meters a.s.l.. Every 6h a new trajectory starts, each trajectory runs 72h.
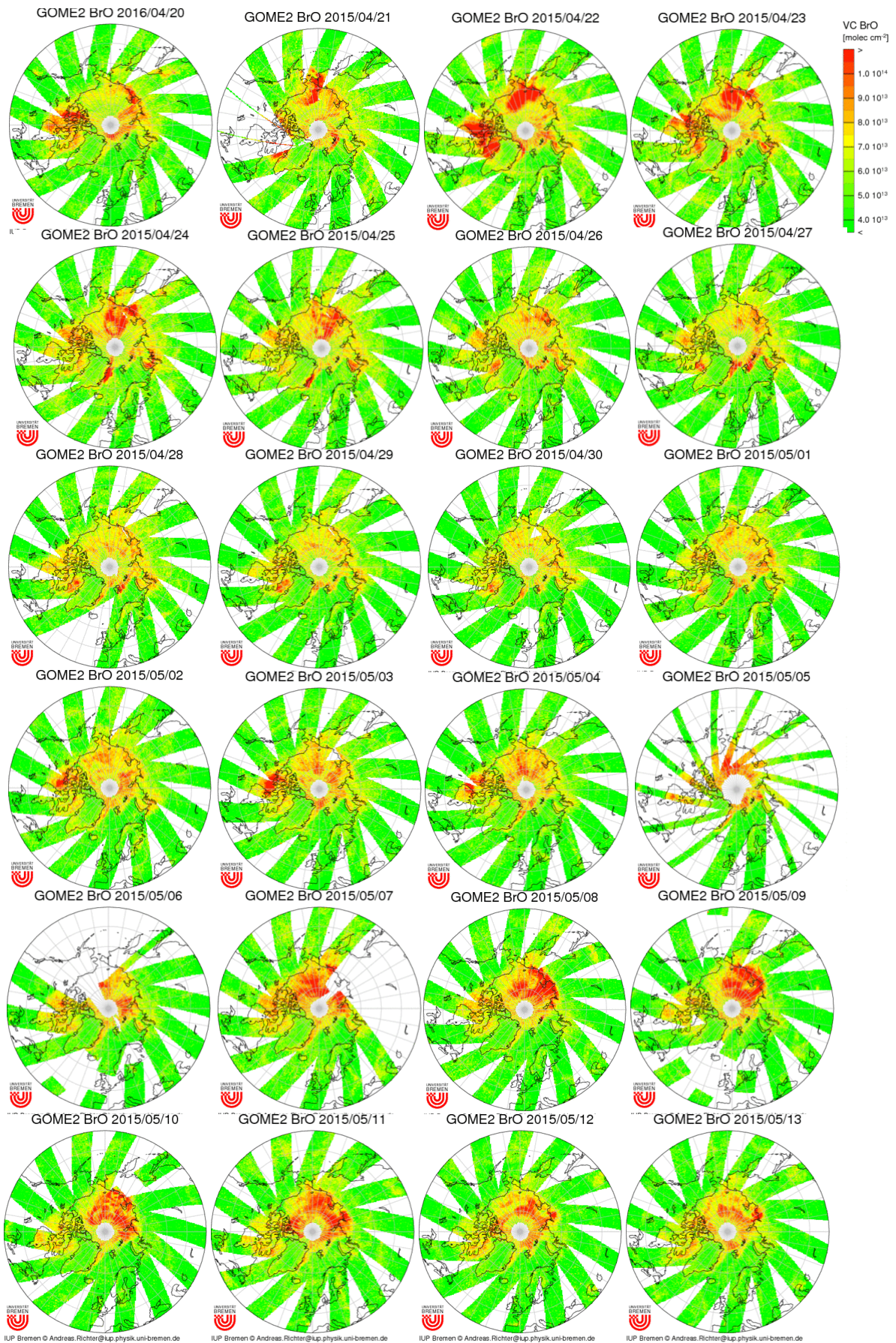
Fig.10 Map of troposphere BrO of northern hemisphere by GOME-2 product from 20 April to 13 May. (Cited from http://www.iup.uni-bremen.de/doas/scia_data_browser.htm)

Fig.11 Sea ice in Kings Bay, Ny-Ålesund at 22:00, 26 April 2015
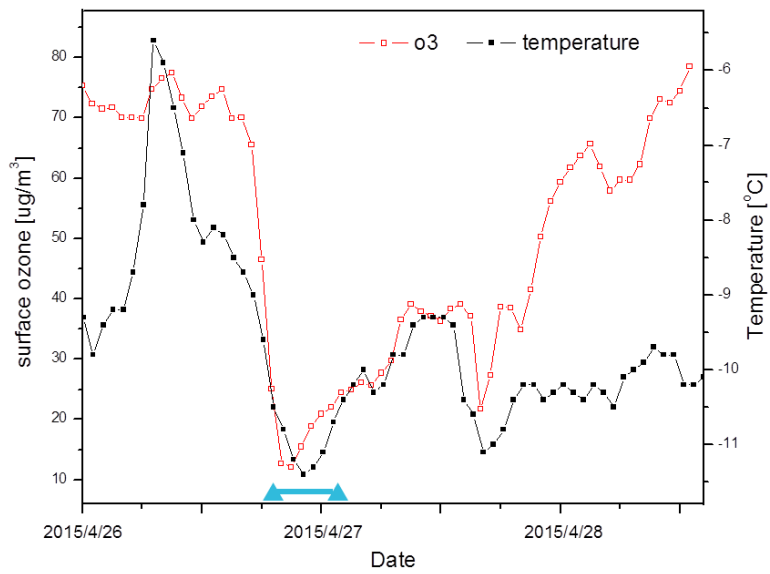
5   **Fig.12 Time series of surface ozone and air temperature during the BrO enhancement event, blue triangles present the sea ice existence in Kings Bay**
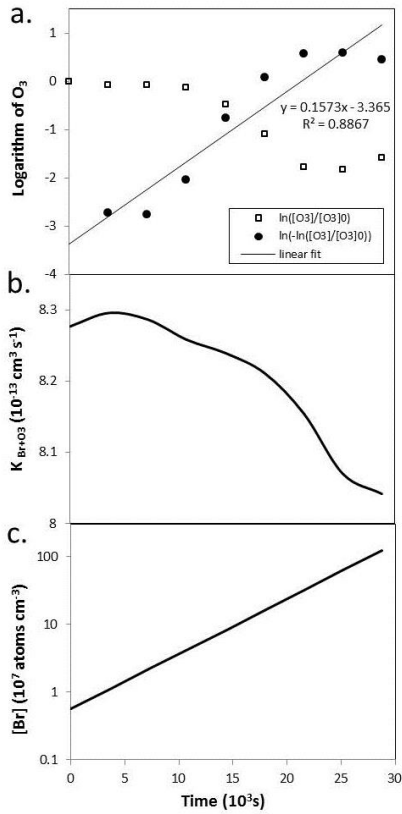
Fig.13 Analysis of surface ozone loss in 26 April 2015

a. Plot of $\ln([O_3]/[O_3]_0)$ and $\ln(-\ln([O_3]/[O_3]_0))$ versus time; b. Calculated temperature dependent reaction rate coefficients for O_3+Br; c. Calculated Br concentration.
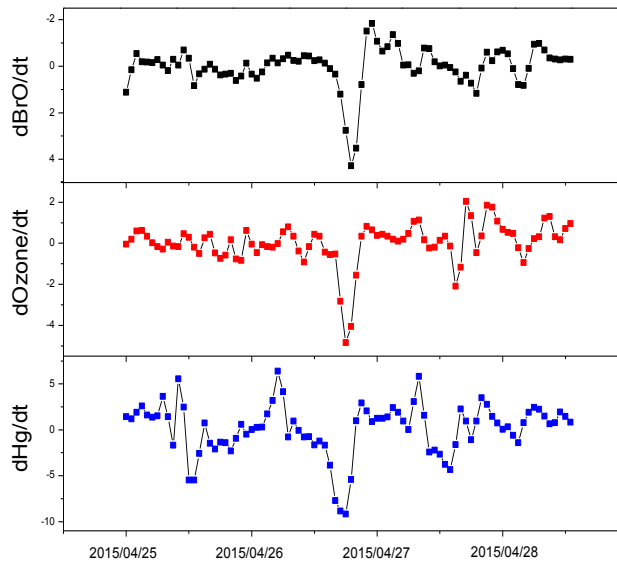
Fig.14 Time series of dBrO/dt, dO3/dt and dHg/dt during the BrO enhancement event